CDF Note 6398

B PHYSICS AT CDF

K. ANIKEEV*

MIT, Fermilab - CDF - MS#318
Batavia, IL 60510-0500
E-mail: anikeev@fnal.gov

B physics is at the core of the CDF agenda for Run II. With the Tevatron performance gradually improving, samples of data corresponding to about $70\,\mathrm{pb}^{-1}$ are now available. Due to improved detector capabilities these data already allow one to improve a number of Run I results, as well as perform a series of new measurements. We present an overview of the current state of B physics at CDF.

1. Introduction

The CDF detector has been upgraded to match the physics goals[1] and to take full advantage of the improved Tevatron performance.[2] Unlike the B factories, B hadrons produced at the Tevatron are not limited to B^+ and B^0, but also include heavier species such as B_s, Λ_b, Ξ_b, *etc.* These latter ones are at the focus of the CDF Run II B physics program. Measurements of mixing and the width difference between CP eigenstates in the B_s system, CKM measurements in $B_s \to J/\psi\phi$ and $B \to h^+h^-$, measurements of masses and lifetimes of B_s, B_c, and Λ_b is just the beginning of the list of exciting results that are expected from Run II.[3]

2. Triggers and Data Samples

An abundant program is enabled by the Tevatron's high CM energy of $\sqrt{s} = 1.96\,\mathrm{TeV}$ and b production cross-section of the order of $0.1\,\mathrm{mb}$. The cross-section for background processes is also very large, about $75\,\mathrm{mb}$, therefore a carefully designed triggering scheme is needed. B physics at CDF relies on three major triggers. These are discussed in the following sections along with the respective data samples and the first Run II results extracted from them.

*On behalf of the CDF collaboration

2.1. *Di-muon Trigger.* J/ψ *Sample*

The di-muon trigger requires two oppositely charged muons with $p_T > 1.5\,\mathrm{GeV/c}$ in the pseudo-rapidity region $|\eta| < 0.6$ or one muon in this η range and the other one in the $0.6 < |\eta| < 1.0$ range with $p_T > 2.2\,\mathrm{GeV/c}$. Most of the di-muons are coming from J/ψ decays, but the contribution from ψ' and Υ is also significant. Thanks to the lower p_T threshold and the increased detector acceptance, the J/ψ yield is up from 2.5 nb in Run I to 7.6 nb in Run II.

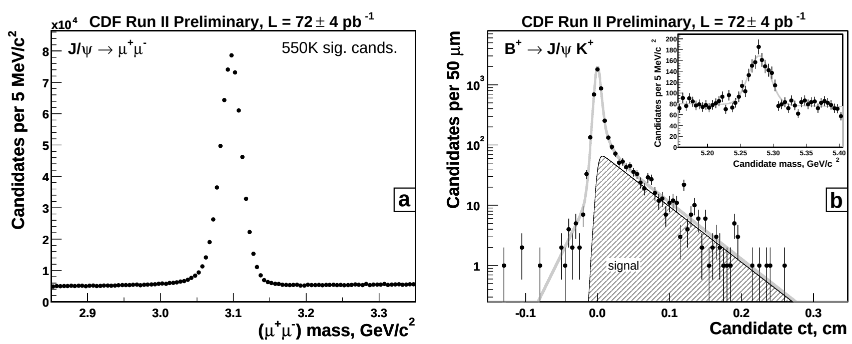

Figure 1. (a) Sample of J/ψ candidates after typical quality cuts are applied. (b) Proper decay length and mass (inlay) distribution with fit results overlaid for $B^+ \to J/\psi K^+$.

A clean J/ψ sample (Fig. 1a) is crucial for detector understanding, but it is also a basis for a number of important physics measurements. Ten to 35% of these J/ψs, depending on p_T, are coming from B decays, such as $B^+ \to J/\psi K^+$, $B^0 \to J/\psi K^{*0}$, $B_s \to J/\psi \phi$, and $\Lambda_b^0 \to J/\psi \Lambda^0$. One can determine the average B lifetime using J/ψ vertices for the transverse decay length measurement and correct $p_T(J/\psi)$ by a Monte-Carlo K-factor for the proper decay length extraction. Using a sample of $18\,\mathrm{pb}^{-1}$, we measured $c\tau_{B_{incl.}} = 458 \pm 10(stat.) \pm 11(syst.)\,\mu\mathrm{m}$, which is in good agreement with the PDG value of $469 \pm 4\,\mu\mathrm{m}$. This large statistics measurement serves as a benchmark of the detector lifetime measuring capabilities.

In the exclusively reconstructed modes mentioned above, one can extract both the lifetime and the mass of the B hadrons. We use a simultaneous maximum likelihood fit to the mass and proper decay length distributions (Fig. 1b) to extract the lifetime. The lifetimes we measure using $72\,\mathrm{pb}^{-1}$ of data are:

$$\tau_{B^+} = 1.57 \pm 0.07\,(stat.) \pm 0.02(syst.)\ \mathrm{ps}$$
$$\tau_{B^0} = 1.42 \pm 0.09\,(stat.) \pm 0.02(syst.)\ \mathrm{ps}$$
$$\tau_{B_s} = 1.26 \pm 0.20\,(stat.) \pm 0.02(syst.)\ \mathrm{ps}$$

In measuring masses one has to account for energy lost by tracks in the material of the detector. One of the difficulties is that the GEANT material map for a detector as complicated as CDF cannot be absolutely complete and accurate. Precise knowledge of the magnetic field is also required. We perform a material and magnetic field calibration using J/ψ (Fig. 2a) and cross-check on Υ which comfortably covers the range of expected B masses. Given the current level of statistics and our understanding of systematic

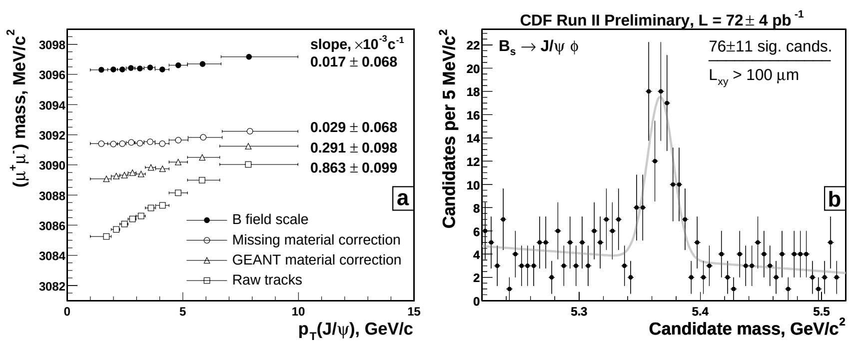

Figure 2. (a) Material and magnetic field calibration using J/ψ. (b) Mass distribution of the $B_s \to J/\psi\phi$ candidates with typical mass measurement cuts (including $L_{xy} > 100\,\mu$m) applied.

effects we expect the world best mass measurements for B_s (Fig. 2b) and Λ_b in the near term future.

2.2. *Displaced Track + Lepton Trigger. $l + D$ Sample*

The displaced track + lepton trigger requires a muon or an electron with $p_T > 4\,$GeV/c and a track with $p_T > 2\,$GeV/c and impact parameter w.r.t. beam line, d_0, satisfying $120\,\mu\text{m} < d_0 < 1\text{mm}$.[4] The data sample obtained with this trigger is therefore enriched in semi-leptonic B decays and is called $l + D$ sample.

There are two primary applications in which $l + D$ sample is used. The first one is development of *flavor taggers*.[3] A tagger is a technical tool, which determines the flavor of b quark at production (whether it was a b or $\bar{b}$). Flavor at decay can usually be inferred from the decay products. Such tools are necessary ingredients for any flavor asymmetry analysis, but as conceived they are not perfect. Each tagger is characterized by two quantities: the efficiency ϵ, and the dilution $D = 1 - 2w$, where w is the mis-tag probability. The error on the asymmetry scales as $1/\sqrt{\epsilon D^2}$, therefore optimizing the taggers, *i.e.* maximizing ϵD^2, is a very important task. Most of the asymmetry measurements will be done in the TTT data sample (Sec. 2.3), therefore $l + D$ is unbiased high statistics sample for tagger optimization.

The other extremely important use of the $l+D$ sample is for measuring lifetimes of B hadrons in their semi-leptonic decays. A clear benefit of this method is large statistics, which is even more important for rare species, such as B_s and Λ_b. The complication of the analysis comes from a non-trivial trigger efficiency w.r.t. the proper decay length resulting from the impact parameter cut described above. CDF uses a realistic Monte-Carlo, that implements all running conditions and weights events by integrated luminosity, to unfold the trigger efficiency from the lifetime measurements.

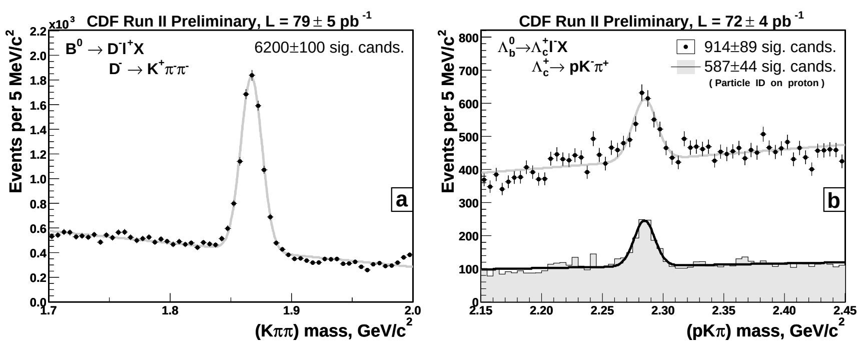

Figure 3. (a) D^- candidates from semi-inclusive reconstruction of $B^0 \to D^- l^+ X$. (b) Λ_c^+ candidates from semi-inclusive reconstruction of $\Lambda_b^0 \to \Lambda_c^+ l^- X$. The shaded histogram shows the same after particle ID (using time of flight and dE/dx information) is required on the proton from Λ_c decay.

Figure 3 shows the mass spectrum of D^- candidates from semi-inclusive reconstruction of $B^0 \to D^- l^+ X$ and the mass spectrum of Λ_c^+ candidates from $\Lambda_b^0 \to \Lambda_c^+ l^- X$. The Run II yields are compared to those from Run I in Table 1. Already at this time CDF has by far the largest in the world samples of semi-inclusively reconstructed B_s and Λ_b.

Table 1. Yield comparison for semi-inclusively reconstructed B hadrons.

Decay mode	Run I (110 pb^{-1})	Run II (~ 70 pb^{-1})
$B^+ \to D^0 l^+ X$	2928 ± 65	$\sim$ 12K
$B^0 \to D^- l^+ X$	1997 ± 65	$\sim$ 6.2K
$B_s \to D_s^- l^+ X$	220 ± 21	~ 600
$\Lambda_b \to \Lambda_c^+ l^- X$	197 ± 25	~ 600

2.3. *Displaced Vertex + High p_T Tracks Trigger. TTT Sample*

The Two Track Trigger (TTT) data sample is accumulated using a trigger which requires displaced high p_T tracks (as described in the beginning of Sec. 2.2) and a secondary vertex. In reality TTT is a combination of triggers with one path optimized for two-body decays like $B \to h_1^+ h_2^-$ and the other one optimized for multi-body decays like $B_{(s)} \to D_{(s)}(3)\pi$. Before this trigger came into existence the only way to control backgrounds in b production was to require leptons, which limited the variety of analyses one could do.

Not only has the advent of the TTT enriched the B program, but also it has opened up charm physics at CDF. In fact, large statistics charm signals were used to understand and tune the trigger and the underlying hardware systems. In the process of doing so a number of precise charm results have been obtained. Using only $10\,\mathrm{pb}^{-1}$ of data, CDF measured the ratios of the branching fraction of the Cabbibo-suppressed decays $D^0 \to KK$, $\pi\pi$ to that of the Cabbibo-favored decay $D^0 \to K\pi$:

$$\frac{Br(D^0 \to K^+K^-)}{Br(D^0 \to K^-\pi^+)} = 11.17 \pm 0.48(stat.) \pm 0.98(syst.)\%$$

$$\frac{Br(D^0 \to \pi^+\pi^-)}{Br(D^0 \to K^-\pi^+)} = 3.37 \pm 0.20(stat.) \pm 0.16(syst.)\%$$

With more integrated luminosity CDF has obtained significant samples of D^*-tagged D^0 and $\overline{D^0}$ decaying into KK and $\pi\pi$ (Fig. 4). These will

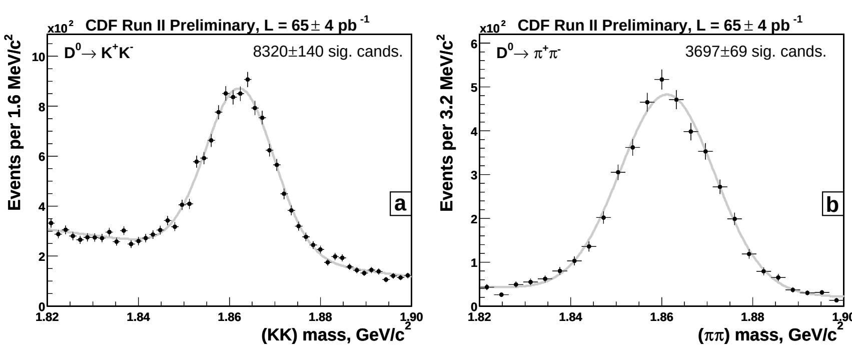

Figure 4. D^0 candidates reconstructed in their decays to: (a) KK, (b) $\pi\pi$.

allow us to substantially improve the precision of the abovequoted ratio measurements, as well as measure direct CP asymmetry, which, if found to be above 1%, would strongly suggest physics beyond the Standard Model.

Another exciting result we obtained from the TTT sample is the measurement of the mass difference between D_s^+ and D^+, which are reconstructed in their decay mode to $\phi\pi$ (Fig. 5a). Common selection and decay kinematics make the systematic uncertainty of this measurement very small. We find[5] $m_{D_s^+} - m_{D^+} = 99.41 \pm 0.38(stat.) \pm 0.21(syst.)$ MeV/c^2, which agrees with the world average and has a similar precision.

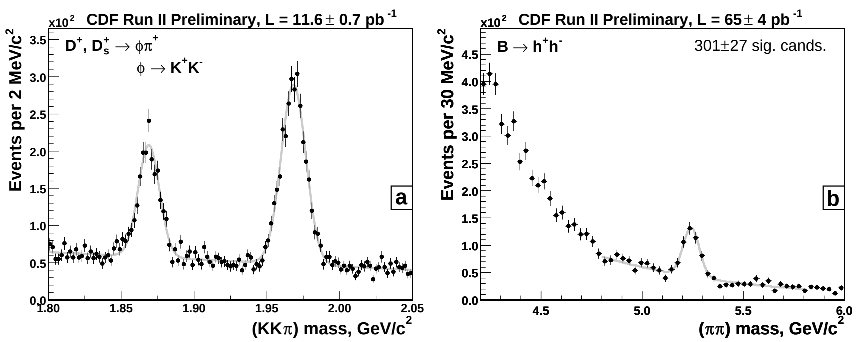

Figure 5. (a) $D_{(s)}^+ \to \phi\pi^+$ candidate invariant mass distribution. (b) $B \to hh$ candidate invariant mass distribution.

Hadronic two body decays $B^0 \to \pi\pi$, $K^+\pi^-$, and $B_s \to KK$, $K^+\pi^-$ will allow us to measure the CKM angle γ. Although these decays have very small branching fractions, CDF has already observed a significant number of them, as shown in Fig. 5b. The width of the mass peak is larger than the detector mass resolution because the peak is a composition of 4 decay modes. A technique to statistically separate these contributions using particle identification with dE/dx is holding promise.

The branching fraction of the decay $B_{(s)} \to D_{(s)}\pi$ is a couple of orders of magnitude higher. In 65 pb^{-1} of data we observe about 500 $B^0 \to D^-\pi^+$ candidates and about 40 $B_s \to D_s^-\pi^+$ candidates (Fig. 6). At present time we pursue the measurement of the ratio of the branching fractions of the two decays, while eventually $B_s \to D_s^-\pi^+$ as well as $B_s \to D_s^-\pi^+\pi^+\pi^-$ will be used to measure B_s mixing.

3. Conclusions

The upgraded CDF detector is back in operation and has accumulated in excess of 70 pb^{-1} of data. Though understanding of the detector is a continuous process, the CDF collaboration is clearly in a phase where competitive analyses can be and already are being done.

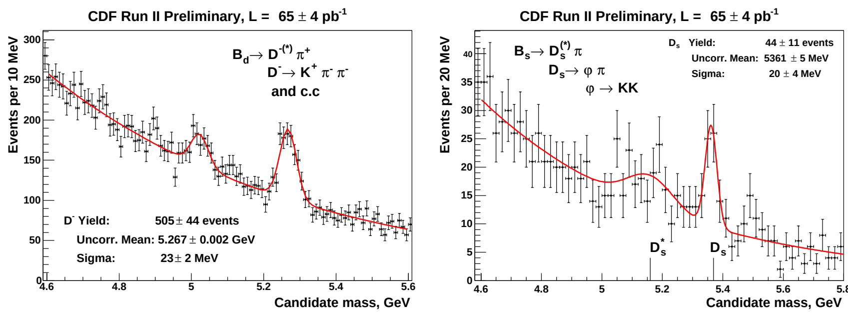

Figure 6. Mass distributions of $B^0 \to D^{(*)-}\pi^+$ candidates and $B_s \to D_s^{(*)-}\pi^+$ candidates.

The majority of the detector systems perform according to or close to the specifications. CDF has already made a number of interesting B physics measurements with Run II data, but many more will surface given a little bit more time and/or increase in total integrated luminosity.

References

1. The CDF II Collaboration, **The CDF II Detector. Technical Design Report**, FERMILAB-Pub-96/390-E (1996)
2. B. Winer, **Recent Results on Top Quark and Electroweak Physics from CDF**, these proceedings
3. K. Anikeev *et al.*, ***B* Physics at the Tevatron: Run II and Beyond** , FERMILAB-Pub-01/197 (2001)
4. A. Bardi *et al.*, Nucl. Instrum. Meth. **A409** (1998) 658
5. The CDF II Collaboration, **Measurement of Mass Difference $m_{D_s^+} - m_{D^+}$ at CDF II** , submitted to Phys. Rev.